THE ARTIFICIAL NEURAL NETWORK AS TECHNIQUE TO SOLVE THE INVERSE PROBLEM OF ELECTROCARDIOGRAPHY: THE EFFECT OF THE TRAINING MARGIN ON THE ERRORS CAUSED BY GEOMETRIC UNCERTAINTIES IN AN ECCENTRIC HOMOGENOUS SPHERICAL MODEL

A.M. Khalifa

Electrical Engineering Department, Faculty of Engineering,
Alexandria University, Alexandria, Egypt.

ABSTRACT

The Artificial Neural Network (ANN) was proved to be useful as a technique to solve the inverse problem of electrocardiography. The training limits of the input data for this problem and the related probability of the output errors are the aim of this paper. Using a model of a homogenous spherical body, the cardiac source was represented by six current dipoles located on the surface of an eccentric heart sphere. Body surface potentials were calculated at 26 measuring points (19x64) cases; representing the all possible combinations of dipoles status (64) in the following (19) cases; The basic case, 8 cases of uncertainty in heart radius r_o , 8 cases of angular uncertainty in θ and 2 cases in Φ of the spherical coordinates. These data were used to train and test the ANN. The obtained results showed that the ANN accepted the training data within a limited margin, beyond which the data would to be contradictory. A zero error margin was obtained within a limited value of the product $\Delta r_o \, \Delta\theta \, \Delta\Phi$. Increasing the safe margin of Δr_o was feasible at the expense of the other margins of $\Delta\theta$ or $\Delta\Phi$. Otherwise, errors would appear inside the margin between the training points.

Keywords : Artificial Neural Network, Inverse Problem of Electrocardiography.

INTRODUCTION

The inverse problem of electrocardiography is to determine the electric activity of the heart from the body surface potential. Several models were constructed to simplify the solution by assuming a regular body shape [1-8]. The complexity of the source was treated as a multipolar [1] or as a multidipolar [2-6] problem. A surface distribution of dipoles was also used [7-8].

The inverse problem was approached by many investigators [2-6]. Gresolwitz and Miller searched for a single moving dipole in a homogenous conductor [9]. Nelson and Hodking [6] assumed two moving dipoles in a circular dish. Oostendorp and Van Oosterom [10] used a nonlinear parameter estimation technique for finding two dipoles inside an inhomogenous volume conductor.

The difficulty of the uniqueness of the solution [11] of the inverse problem of electrocardiography, directed the attention of many investigators to the recovery of the epicardial potential from the body surface potential [12]. Body surface Laplacian ECG mapping was recently introduced to give better information about the cardiac events [13-14]. Ill-posedness and regularization of the inverse problem was discussed in many recent publications [15-19].

The ANN as a technique to solve the inverse problem of electrocardiography was previously proposed by the author of this paper [20] for the following advantages:
I) the nonlinear nature of the inverse problem, and II) the fast response of the ANN as a practical need for this problem.

In the present work we tried to feed the ANN with a relatively large data size related to all possible combinations of cardiac dipoles status with a wide range of geometric uncertainties. The aim of this study was to find the maximum size of the training margin and the relationship between the training margin and the probability of errors for the problem under consideration.

MODEL DESCRIPTION AND POTENTIAL CALCULATIONS

A homogenous spherical model of radius R is employed to represent the body in the present study (Figure 1). The cardiac electric activity is represented by 6 current dipoles located on the surface of an eccentric cardiac sphere of radius r_o = 0.4R and eccentricity ε = 0.4R . The dipoles are oriented in the radial direction with respect to the cardiac center o' . This configuration resembles the activation areas in the basal-apical, right-left, and frontal-rear directions.
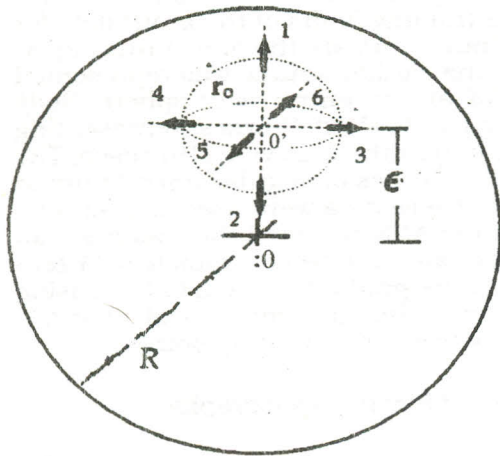

Figure 1 The cardiac electric activity is represented by 6 current dipoles. The heart is an eccentric sphere with radius r_o and eccentricity ε inside a spherical body of radius R.

The surface potential $V_{sz}(\theta)$ produced by a unit current dipole oriented in the Z-direction and located at r, is given by[15]

$$v_{sz}(\theta) = \frac{1}{4\pi\sigma R^2} \sum_{n=1}^{\infty} (2n+1)(\frac{r}{R})^{n-1} P_n^0(\cos\theta) \qquad (1)$$

while for a dipole pointing to X-direction, the surface potential $V_{sx}(\theta, \Phi)$ is given by [15]:

$$V_{sx}(\theta,\phi) = \frac{1}{4\pi\sigma R^2} \sum_{n=1}^{\infty} (\frac{2n+1}{n})(\frac{r}{R})^{n-1} P_n^1(\cos\theta) \qquad (2)$$

where; σ is the body conductivity, P_n^0 & P_n^1 are the Legender polynomials of zero and first order.

Equation 1 was used directly to give the potential produced by either dipoles no.1 or 2 . While for dipole no. 3 , we considered its two components (r ,and θ directions). Body surface potentials due to these components were calculated utilizing equations (1) and (2) after rotating the coordinates. Same procedures where done for dipoles no. 4,5, and 6.

All possible combinations of the 6-dipoles were considered and their corresponding potential functions $V_s(\theta,\Phi)$ were calculated. Potential values for 26 measuring nodes (Figure 2) were calculated and stored. Similar to the measuring system of the human electrocardiography the surface nodes were located at the frontal half of the sphere (ϕ=0 -to- π). Eight points were located on each half ring ($\theta=\pi/4$, $\pi/2$ and $3\pi/4$) and the rest two points were the top and bottom of the sphere.
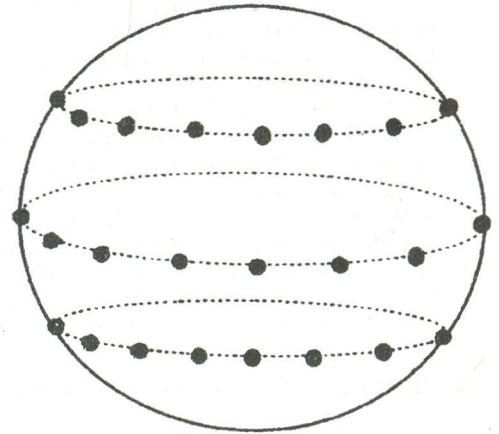

Figure 2 The 41 measuring points on the frontal half of the spherical body.

For the basic case, with r_o = 0.4R and ε = 0.4R , potentials (26 points) were calculated for all possible combinations (64) of the six dipoles. The 64 cases were repeated for different values of r_o/R = 0.3, 0.33, 0.35, 0.37, 0.43, 0.45, 0.4, and 0.5 .
Also, calculations were done for angular shifts $\Delta\theta$ = ±4°, ±8°, ±10°, and ±12°, and for $\Delta\phi$= ±15°. This gave us a data base of size 26x64x19. Some of these cases were plotted in Figure 3.

TRAINING OF THE ANN

The back propagation is a well known optimization method in ANN learning techniques. Such algorithm is designed to minimize the difference between the actual output of a multi-layered feed forward network and the desired output. In this algorithm the output Z_i of a given i_{th} node is a
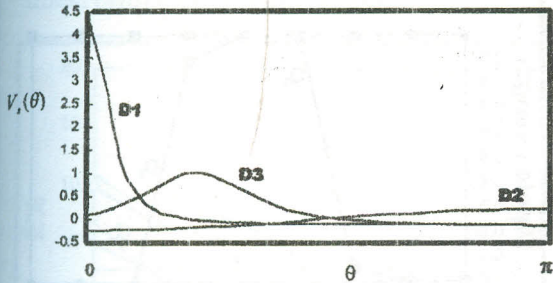
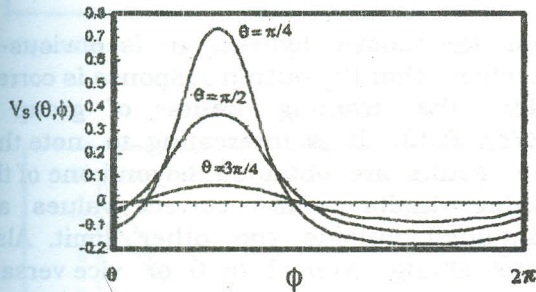**Figure 3-a** The surface potential $V_s(\theta)$ produced by the current dipoles Nos.. 1, 2 and 3.

Figure 3-b The surface potential $V_s(\theta,\phi)$ produced by the current dipole No. 5.

Figure 4-b A diagram illustrating the three layers of the ANN: the input, the output and the hidden layer.

weighted sum of its inputs Y_i (Figure 4) according to:

$$Z_i = f(\sum_{j=1}^{N} W_{ij} y_i + b_i) \qquad (3)$$

where:

W_{ij} are weight constants,
f is a nonlinear sigmoid function defined as :

$$f(x) = \frac{1}{1 - e^{-x/T}} \qquad (4)$$

where:

T is called the temperature parameter that controls the nonlinearity of the functions
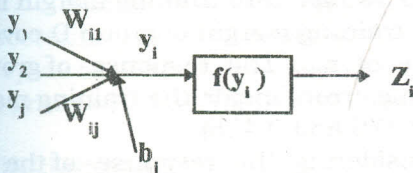

Figure 4-a The output Z_i of an ith node is a weighted sum of its inputs Y_i, through a nonlinear function f.
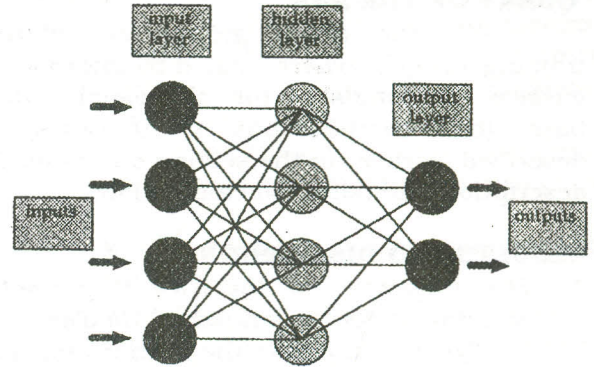
In our problem, we used the NCS package to design and train a suitable system. The system consisted of three layers; an input, an output and a one hidden layer (Figure4). The number of nodes was 26 according to the number of the measuring points. The output nodes were 6 representing the heart dipoles. The number of nodes of the hidden layer was 300, which had been selected according to several trials.

The system was trained by using the 26 potential values as inputs and the corresponding status of the dipoles (1/0) as output. In order to test the learning ability or the training margin of the proposed system, the learning data was divided into 4 groups; A,B,C, and D.

Group A: included only the basic problem , where the dipoles were located at $r_o = 0.4R$, without any shift in θ or ϕ . This group consisted of 64 different combinations of dipoles status.

Group B: included the 64 combinations of the dipoles status in 7 cases. Three of them corresponded to $r_o/R = 0.4, 0.35$, and 0.45 (without any shift in θ or ϕ), and the other 4 cases corresponded to a shift $\Delta\theta = \pm 8°$, and $\Delta\phi = \pm 15°$ (with $r_o/R=0.4$).

Group C: Same as B, but for the following 7 cases; $r_o/R = 0.4, 0.37$, and 0.43 (without any shift in θ or ϕ), and $\Delta\theta = \pm 4°$, and $\Delta f = \pm 15°(r_o/R = 0.4)$.

GroupD: included only 5 cases; $r_o/R = 0.35$, 0.37, 0.4, 0.43, and 0.45 ($\Delta\theta = 0°$, and $\Delta\phi = 0°$).

QUERY OF THE ANN

All the above groups of different training criteria where tested by intering the surface potentials of the all available data base (64 combinations x 19 cases) as described earlier in the section on the model description and potential calculation.

RESULTS AND DISCUSSION

A- *The response of the ANN to geometric uncertainty for the individual dipoles*:

Figure 5-a shows the output response of the ANN for D_6 and D_5. The input data were chosen from the calculated data base for cases where $D_6=1$ with all other dipoles of zero value . This selection covered all the cases of r_0/R uncertainties from $r_0/R = 0.3$ to 0.5 (Group C).

Results showed a correct output for D_6 for $r_0/R>0.375$, and a false zero for $r_0/R < 0.35$. Also, a false positive result was obtained for D_5 for $r_0/R<0.33$ and a correct zero for greater values of r_0/R .

Same procedure was repeated except that the input data were belonging to $D_6=1$, with all other dipoles = 1. Similar response for D_6 was obtained as seen in Figure 5-b. But for D_5 a correct value of 1 was obtained for $r_0/R \leq 0.43$,and a false zero for $r_0/R > 0.45$.
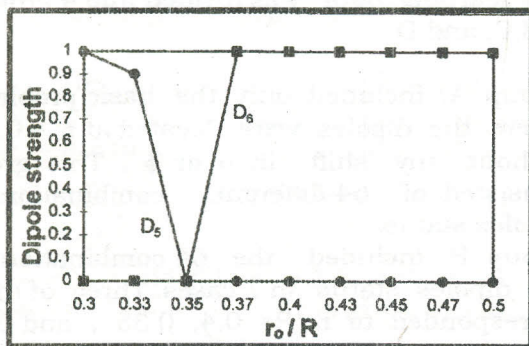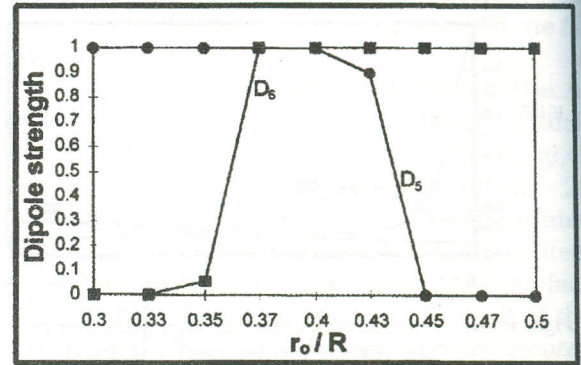

Figure 5-b   Same as Figure 5-a, but for input data corresponding to all dipoles D_1 to D_6 having a unity value.

From the above figures, it is obvious-as expected- that the output response is correct within the training limits of group C $(0.37 \leq r_0 \leq 0.43)$. It is interesting to note that false results are obtained beyond one of the training limits while correct values are maintained outside the other limit. Also, abrupt change from 1 to 0 or vice versa is noticeable.

B- *The effect of the training margin on the response of the ANN to geometric uncertainty* :

Figure 6-a shows the statistical error function as a response of the ANN to the uncertainty in the heart radius r_0/R (from 0.3 to 0.5) for the different training groups A,B,C, and D. The statistical error is calculated as the number of false output N_F (1,0, or undefined values) divided by the total number of dipoles status in each case(64 x 6). Accordingly the percentage statistical error E = $(N_F$ x 100)/ (64 x 6). It is obvious from this figure, that group A gives the higher values of errors, while group D shows an optimum response to the uncertainty of r_0 . This is an expected result, specially when we consider that group A has zero training margin in r_0 , while the training margin of group D covers a wide range of r_0 . The response of group B shows some errors inside the training margin (at $r_0/R= 0.375$ and 0.425).

Considering the response of the ANN to the uncertainty in θ and ϕ of the dipoles orientations, the results are shown in Figure 6-b. Comparing the results of groups B and C, it is obvious that increasing the range of training in B creates inter range errors, which

Figure 5-a   The strength of dipoles D_5 and D_6 as outputs of the ANN. The input data was obtained from forward calculations of the body surface potential produced by the dipole $D_6=1$ located at the different positions (r_0/R). All other dipoles D_1 to D_5 were set to zero. This output was obtained from the ANN (Group C). False results for both D_5 and D_6 are observed for $r_0/R < 0.37$

is very similar to the results obtained for uncertainty of r_o (Figure 6-a).
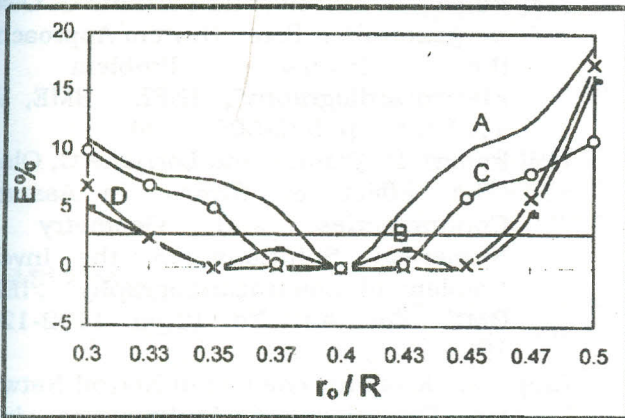

Figure 6-a The percentage statistical error E for the ANN output as a response to the uncertainity of the heart size r_o/R for the different training groups A, B, C, and D.
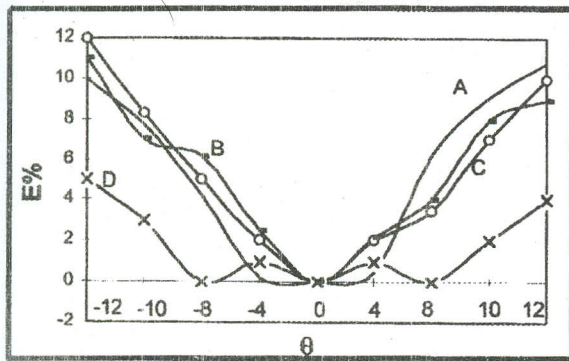

Figure 6-b Same as Figure 6-a, but with the uncertainity of the dipoles orientation in

Also, the group A, with zero training range, gives high errors with the uncertainty in θ.

As a complementary result to Figure 6-a group D, which has a wide range of training in r_o and zero training range in θ, gives high error response as indicated in Figure 6-b. Also, group C has an optimized error free range in both Figures 6-a and 6-b.

Similar results were expected with the uncertainty in ϕ. Therefore, we preferred to keep a constant training margin in $\phi(\Delta\phi = \pm15°)$ for groups B&C, and $(\Delta\phi= 0°)$ for groups A&D.

CONCLUSIONS

The ANN can be successively used to solve the inverse problem of electrocardiography with the following considerations:

a- For the ANN, there should be a training margin for the geometric parameters to overcome the problem of geometric uncertainties in the inverse problem of electrocardiography.

b- It is not possible to increase the training margin for all parameters because of their contradictory effect.

c- A wide training margin may create inter-range errors.

d- Increasing the training margin for one parameter is limited by the increased errors associated with the other parameters.

e- An optimization should be done between the margins of the different parameters according to the expected uncertainties of each one.

f To cover wide ranges of uncertainties for all parameters, a multi-ANN system with different training margins can be used for the same problem with a special device for output selection.

REFERENCES

[1] R.M. Arthur, "Quadrupole Components of the Human Surface Electrocardiogram" Am. Heart. J., Vol. 83(5), pp.633-677, 1972.

[2] E.S. Fishmann and Barber "Aimed Electrocardiography: Model Studies Using A Heart Consisting of 6 Electrical Areas"; Am. Heart J., Vol. 65, pp. 628 - 637, 1963.

[3] J.H. Holt "A Study of the Human Heart As A Multiple Dipole Electrical Source :I- Normal Adult Male Subject", Circulation, Vol. XI, pp. 687-696, 1969.

[4] J.H. Holt "A Study of the Human Heart As A Multiple Dipole Electrical Source : II- Diagnosis and Quantitation of left Ventricular Hypertrophy", Circulation ,Vol. XI, pp. 697-710, 1969.

[5] A. Stewart Ferguson and G. Stroink, "The Potential Generated By Current Sources Located In An Insulated Rectangular Volume Conductor", J.Appl. Phys. Vol. 76, No. 12, pp. 7671-7676, 1994.

[6] C.V. Nelson, and B.C. Hodking "Determination of Magnitudes, Directions And Locations of Two Independent Dipoles In A Circular Conducting Region From Boundary Potential

Measurements", IEEE, BME - Vol. 28, No. 12, pp. 817-823, 1981.

[7] Y. Rudy and Plonsey, "A Comparison Of Volume Conductor And Source Geometry Effects On Body Surface And Epicardial Potentials", Cir. Res. Vol. 46, pp. 328-331, Feb. 1980.

[8] Y. Rudy and R. Plonsey, "The Eccentric Spheres Models As the Basis For Study of the Role of Geometry And Inhomogenities In Electrocardiography", IEEE, BME, Vol. 26, No. 7, pp. 392-399, 1979.

[9] Walter R. Miller and David B. Geselowitz, "Simulation Studies of the Electrocardiogram :1. The Normal Heart". Circ. Res., Vol. 43, pp.301-314, 1978.

[10] Thom F. Oostendorp and Adrian Van Oosterom, "Source Parameters Estimation in Inhomogeneous Volume Conductors of Arbitrary Shape", IEEE, BME, Vol. 36, No. 3, pp. 382-391, 1989.

[11] Yasuo Yamashita, "Theoretical Studies On The Inverse Problem In Electrocardiography And the Uniqueness of the Solution", IEEE, BME, Vol. 29, No. 8, pp. 719-725, 1982.

[12] B.J. Messinger, Y. Rudy, "The Inverse Problem in Electrocardiography: A Model Study of the Effect Epicardial Potentials", IEEE, BME, Vol. 33, No. 7, pp. 667-676, 1985.

[13] Bin HE and Richard J. Cohen. "Body Surface Laplacian ECG Mapping", IEEE, BME, Vol. 39, No. 11, pp. 1179-1191, 1992.

[14] Thom F. Oostendorp and Adrian Van Oosterom, "The Surface Laplacian of the Potential: Theory and Application", IEEE, BME, Vol. 43, No. 4, pp. 394-405, 1996.

[15] Mario Bertero, Tomaso A.poggio, and Vincent Torr, "Ill-Posed Problems in Early Vision", Proceedings of the IEEE, BME, Vol. 76, No. 8, pp. 869-889, 1988.

[16] Haward S. Oster, and Yoram Rudy, "The Use of Temporal Information in Regularization of the Inverse Problem of Electrocardiography", IEEE BME, Vol. 39, No. 1, pp. 65-75, 1992.

[17] Vahid Shahidi, Pierre Savard, and Reginald Nadeau, "Forward and Inverse Problems of Electrocardiography: Modeling Recovery of Epicardial Potentials in Humans ", IEEE, BME, Vol. 41, No. 3, pp. 249-256, 1994.

[18] Robert D. Throne, and Lorriane G. Olson, "a generalized Eigen System Approach to the Inverse Problem of Electrocardiography", IEEE, BME, Vol. 41, No. 6, pp. 592-600, 1994.

[19] Robert D. Throne, and Lorriane G, Olson, "The Effect of Errors in Assumed Conductivities and Geometry on Numerical Solutions to the Inverse Problem of Electrocardiography", IEEE, BME, Vol. 42, No. 12,pp. 1192-1200, 1995.

[20] A.M. Khalifa, "The Use of Neural-Network for Detection of Multidipoles in a Homogeneous Spherical Conductor: A Proposed Technique for The Inverse Problem of Electrocardiography", ECSAP, pp. 395-399, Prague 1997.